On the regime of validity of sound-proof model equations for atmospheric flows

Rupert Klein

FB Mathematik & Informatik, Freie Universität Berlin
Arnimallee 6, 14195 Berlin, Germany
E-mail: rupert.klein@math.fu-berlin.de

ABSTRACT

This paper summarizes, and slightly extends, the key results of two recent publications (Klein et al., JAS, 2010 and Achatz et al., JFM, 2010).

Soundproof atmospheric flow models are considered attractive for two reasons: (i) Since acoustic modes are likely of negligible influence in atmospheric dynamics, sound-proof models have the advantage of a clear-cut focus on the essentials of such flows. (ii) Although several numerical schemes for the compressible atmospheric flow equations are being used in production codes, uncertainties w.r.t. their robustness, accuracy, or flexibility remain.

Ogura and Phillips' (1962) derivation of their anelastic model requires the dimensionless stability of the background state to be of the order of the Mach number squared, i.e., $(h_{\rm sc}/\overline{\theta})\,d\overline{\theta}/dz = \mathscr{O}(\varepsilon^2)$ as $\varepsilon \to 0$. This guarantees the characteristic time scales of advection and internal waves to be of the same order of magnitude in the Mach number, ε. Assuming the flow evolution to develop on this time scale only, they asymptotically eliminate the fast sound waves and arrive at the anelastic model featuring internal waves and advection only. For typical values $\varepsilon \sim 1/30$, however, the model implies unrealistically weak vertical variation of potential temperature across the troposphere of less than one Kelvin. Later generalizations of the anelastic model (Dutton & Fichtl (1969), Lipps & Hemler (1982)), and Durran's pseudo-incompressible model (Durran 1989) are argued to be valid for stronger stratification, yet their derivations do not account for the fact that one must deal with three separated time scales for sound, internal waves, and advection in this case.

Klein et al. (2010) address this issue and show that the Lipps & Hemler anelastic model and Durran's pseudo-incompressible model should be valid up to stratifications $(h_{\rm sc}/\theta)\,d\theta/dz < \mathscr{O}(\varepsilon^{2/3})$ corresponding to vertical variations of potential temperature of $\Delta\theta\,\big|_0^{h_{\rm sc}} < 30...50$ K. Achatz et al. (2010) study, *i.a.*, the evolution of large amplitude, short wave internal wave packets using WKB theory. They show that the pseudo-incompressible model is asymptotically consistent with the compressible Euler equations even for leading-order stratifications in the considered WKB regime. In contrast, they find this not to be true for the Lipps & Hemler anelastic model, whose asymptotics differs in the first-order terms. We show in the present paper that the anelastic model does correctly represent the amplification of wave packets as they travel upwards in the atmosphere, but that the excitation of higher harmonics and the wave-meanflow-interactions are not consistent with the asymptotics of the compressible Euler and pseudo-incompressible models.

1 Introduction

1.1 Why don't we "simply" solve the compressible flow equations?

The numerical approximation of the nonlinear advection terms in the compressible or sound proof flow equations is computationally expensive, especially when multiple advected species need to be accounted for. It is thus desirable to invoke these advection schemes no more often than needed to achieve the targeted advection accuracy, i.e., at effective advection CFL numbers of order unity. Two types of approaches to such large time step methods are currently implemented in production codes: split explicit

and semi-implicit schemes (see, e.g., Klemp et al., 2007; Jebens et al., 2009; Reich, 2006; Durran, 2010, and references therein).

We concentrate here on semi-implicit methods, which are designed to allow for time steps corresponding to large acoustic, but order unity advective CFL numbers. One principal potential problem with such schemes is elucidated in Fig. 1. We have solved the, appropriately non-dimensionalized, linear acoustic equations

$$u_t + p_x = 0\,, \qquad p_t + u_x = 0 \tag{1}$$

on $x \in [-1/2, 1/2]$, with periodic boundary conditions, and simple wave initial data

$$\begin{aligned} u(0,x) &= U\left(\exp\left(-\left[\tfrac{x-x_1}{\sigma}\right]^2\right) + \exp\left(-\left[\tfrac{x-x_2}{\sigma}\right]^2\right)\cos\left(2\pi\tfrac{x-x_2}{\ell}\right)\right)\,, \\ p(0,x) &= u(0,x)\,, \\ [U, x_1, x_2, \sigma, \ell] &= [1, 0.25, -0.25, 1/10, 1/70]\,, \end{aligned} \tag{2}$$

using the implicit midpoint rule. This is an energy preserving symplectic second order accurate solver, which should thus be well suited for solving problems with long-time oscillatory solutions, (Hairer et al., 2006).

The figure shows the pressure distributions at times $t = 0$, $t = 2.5$, and $t = 3$. In the exact solution, the initial distribution moves to the right, passes the domain three times, and by time $t = 3$ has returned to its initial position. Thus, for the exact solution the distributions at the top and bottom of Fig. 1 would be indistinguishable. As becomes evident from the middle figure ($t = 2.5$), the modulated short wave packet is almost stationary in the numerical solution, whereas the long wave pulse starting out at $x = 0.25$ is moving at roughly the correct speed while being distorted by weakly dispersive effects.

We conclude that the implicit midpoint rule achieves its unconditional stability w.r.t. the CFL number by slowing down the rapidly oscillating modes, while maintaining the mode amplitudes. In the context of a full-fledged semi-implicit atmospheric flow solver, such behavior would be dangerous in the following way. Any small scale disturbance induced, e.g., by the action of subgrid scale parameterizations would be interpreted, at least partially, as short wave sound by the discretization with its amplitude maintained in time. As time progresses, such short wave perturbations can amplify and generate an entirely unphysical distribution of potentially amplifying, nearly stagnant fake acoustic patterns.

There are various remedies to this problem, such as sacrificing second order accuracy and "off centering" of the time discretization (this corresponds roughly with blending the implicit midpoint rule and the first order accurate implicit Euler method), or adopting dissipative numerical schemes such as BDF2 (backward differencing formula, second order). Yet, as long as the way in which such schemes control the underresolved acoustic modes and their interaction with diabatic subgrid scale parameterizations is not clarified analytically, there remains an uncertainty regarding how such interactions may affect atmospheric flow integrations over thousands of time steps.

An alternative that obviously does guarantee the absence of fake sound modes in atmosphere simulations consists of adopting a sound-proof flow model in the first place. Here, however, one must understand the regime of validity of such models, and this is what is discussed in this paper

1.2 Anelastic and pseudo-incompressible models

1.2.1 Design regime

Ogura and Phillips (1962) derived the original anelastic model through systematic formal asymptotics using the flow Mach number as the expansion parameter, so that $M = \varepsilon \ll 1$. To arrive at a reduced model that would have internal waves and advection feature comparable time scales, Ogura and Phillips had to adopt a distinguished limit stating that the dimensionless stability of the background state be of the order

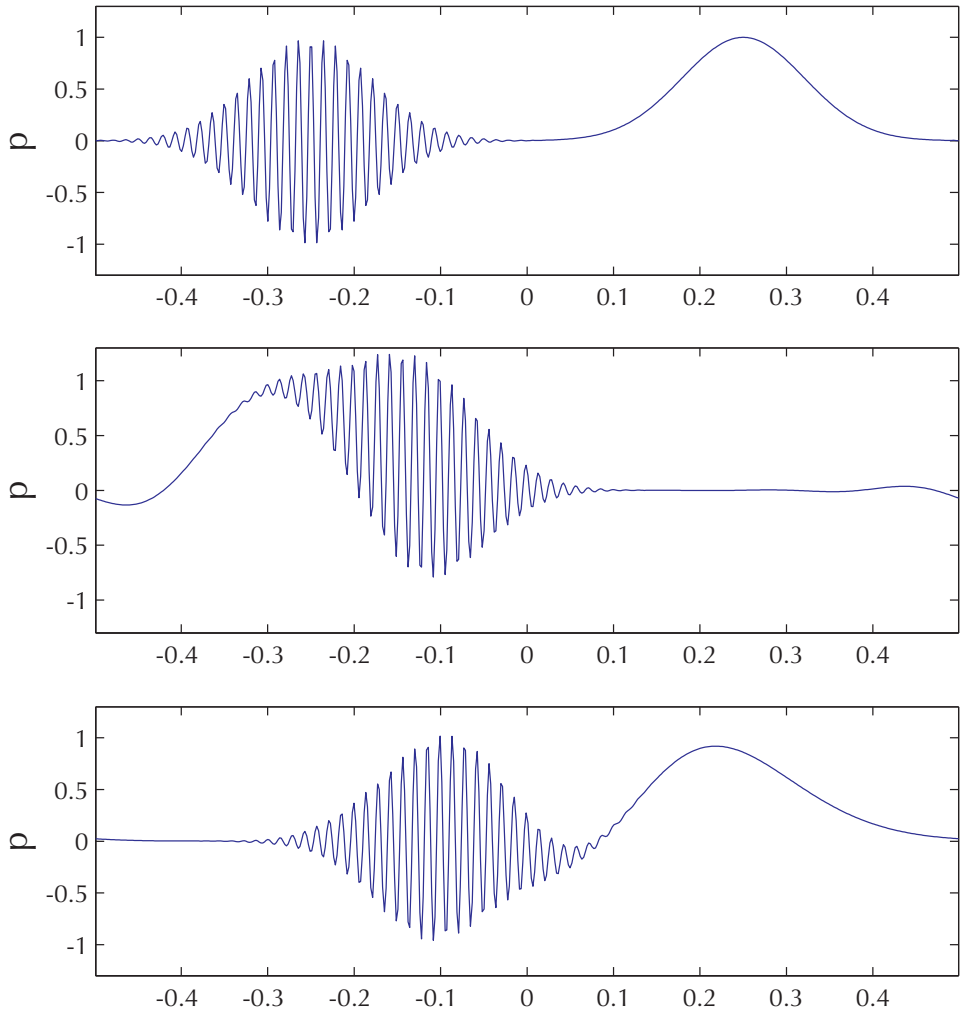

Figure 1: Initial data (top) and numerical solutions on 512 grid cells with CFL $= 10$ *based on the implicit midpoint rule at times* $t = 2.5$ *(middle) and* $t = 3$ *(bottom) for the linear acoustics test from (1), (2)*

Table 1: Characteristic inverse time scales

		dimensional	dimensionless
advection	:	$\frac{u_{\rm ref}}{h_{\rm sc}}$	1
internal waves	:	$N = \sqrt{\frac{g}{\overline{\theta}}\frac{d\overline{\theta}}{dz}}$	$\frac{\sqrt{gh_{\rm sc}}}{u_{\rm ref}}\sqrt{\frac{h_{\rm sc}}{\overline{\theta}}\frac{d\overline{\theta}}{dz}} = \frac{1}{\varepsilon}\sqrt{\frac{h_{\rm sc}}{\overline{\theta}}\frac{d\overline{\theta}}{dz}}$
sound	:	$\frac{\sqrt{gh_{\rm sc}}}{h_{\rm sc}}$	$\frac{\sqrt{gh_{\rm sc}}}{u_{\rm ref}} = \frac{1}{\varepsilon}$

of the Mach number squared. For typical flow Mach numbers of $\varepsilon \sim 1/30$ this amounts to total variations of potential temperature across the troposphere of less than one Kelvin, i.e., to unrealistically weak stratification. Various generalizations of the original anelastic model have been proposed to remedy this issue, e.g., by Dutton & Fichtl (1969), and Lipps & Hemler (1982). Durran (1989) proposed the pseudo-incompressible model following the same goals, but a somewhat different route of argumentation.

Sound-proof models should describe atmospheres vertically covering at least a typical pressure scale height, $h_{\rm sc} \sim 10$ km, and non-hydrostatic flow regimes with horizontal scales down to 10 km or less (cf., Bannon, 1996). Thus the characteristic vertical as well as horizontal length scales for the design regime of these models are comparable to the pressure scale height, $h_{\rm sc}$. Table 1 displays the inverse characteristic times of sound propagation, internal waves, and advection in dimensional and non-dimensional form. The formulae reveal that an asymptotic single time scale model which resolves the advection time scale and includes internal waves at the same time must involve weak stratifications, $(h_{\rm sc}/\theta)\, d\theta/dz = O(\varepsilon^2)$, in line with Ogura and Phillips' argumentation. For typical flow Mach numbers of $\varepsilon \sim 1/30$ such stratifications amount to total variations of potential temperature across the troposphere of less than one Kelvin, i.e., to unrealistically weak stratification as discussed above. According to Table 1 any stronger stratification with

$$\frac{h_{\rm sc}}{\theta}\frac{d\theta}{dz} = O(\varepsilon^{\mu}) \qquad \text{where} \qquad 0 < \mu < 2 \tag{3}$$

will induce a three–time scale asymptotic limit so that

$$t_{\rm ac} \ll t_{\rm int} \ll t_{\rm adv} \qquad \text{with} \qquad t_{\rm ac} = O(\varepsilon\, t_{\rm adv})\,, \quad t_{\rm int} = O(\varepsilon^{1-\mu/2}\, t_{\rm adv})\,. \tag{4}$$

Sound-proof models derived for such a regime of stratifications will thus constitute asymptotic two-scale models in time, retaining a scale separation between the internal and advection time scales. In deriving their models, Dutton and Fichtl (1969), Lipps and Hemler (1982), Durran (1989), and Bannon (1996) provide a range of physical arguments for their validity. Yet, the two–time scale nature of the resulting sound-proof models for stratifications within the regime from (3) is not addressed. Neither have we found the internal–wave/Lagrangian time scale separation addressed in more recent scaling or asymptotic analyses of Davies et al. (2003) and Almgren et al. (2006). At the same time, numerical experience indicates that sound-proof models work well on a much broader range of scales and problems than would be anticipated based on theoretical arguments (cf. Prusa et al., 2008, and references therein).

The presence of multiple scales in the sound-proof models is, nevertheless, an issue, because both the spatial structures and frequencies of internal waves featured by the sound-proof models only approximate those represented by the full compressible flow equations. As a consequence, there are two necessary conditions for the validity of the sound-proof models over the targeted advective time scales: (a)

the spatial structures of corresponding internal wave eigenmodes of the sound-proof and compressible systems should be asymptotically close as $\varepsilon \to 0$; and (b) the accumulation of phase differences between such sound-proof and compressible internal waves should remain asymptotically small at least over the advective time scale.

Motivated by these considerations, Klein et al. (2010) consider atmospheres with stratifications in the regime from (3), compare the internal wave eigenmode structures of the compressible Euler equations and selected sound-proof models, assess the approximation errors due to "sound-proofing" for both the spatial eigenmodes and the associated frequencies in terms of the Mach number, and demonstrate that internal wave solutions of the sound-proof and compressible models remain asymptotically close for $t = O(t_{\rm adv})$ for sufficiently weak stratification. Specifically, for both Lipps & Hemler's and Durran's sound-proof models they find a corresponding bound on the stratification,

$$\frac{h_{\rm sc}}{\theta}\frac{d\theta}{dz} = O(\varepsilon^{\mu}) \qquad \text{with} \qquad \mu > \frac{2}{3}. \tag{5}$$

This corresponds to realistic stratifications with $\Delta\theta\,|_0^{h_{\rm sc}} = 30...50$ K over 10...15 km.

1.2.2 Large amplitude internal wave packets

Being interested in the breaking of relatively short wave internal waves at high altitudes in the stratosphere, Achatz et al. (2010) refine existing WKB theories to cover large amplitude internal wave packets with characteristic lengths $\ell \ll h_{\rm sc}$, which may travel over distances comparable to the potential temperature scale height, i.e., $L \sim H_\theta$. We note that for weak stratification one has, $H_\theta \gg h_{\rm sc}$, while for order one stratification, $H_\theta \sim h_{\rm sc}$. The study shows that Durran's pseudo-compressible model has the exact same leading and first order accurate large amplitude WKB theory as the full compressible flow equations no matter what is the background stratification. In contrast, for the Lipps & Hemler anelastic model there is a difference in the first order asymptotics involving – not surprisingly – the velocity divergence. Achatz et al. (2010) show explicitly that the excitation of higher harmonics and the wave-mean flow interaction terms differ for the anelastic model.

In the present paper we compare the WKB expansions for the Lipps-Hemler anelastic and pseudo-incompressible models and show that – somewhat surprisingly – they do not differ with respect to the amplification of a wave packet as it travels vertically in the atmosphere to regions of low density, even though this is a first-order effect. The reason is some subtle cancellation associated with the simultaneous change from one model to the other of both the nonlinear pressure gradient terms in the momentum equations and the divergence constraint.

1.3 Structure of this paper

Section 2, following (Klein et al., 2010), discusses asymptotic constraints on the validity of the Lipps & Hemler anelastic and pseudo-incompressible models in their design regime, which involves horizontal and vertical length scales comparable with the pressure scale height (≈ 10 km) and time scales up to and including the associated characteristic advection time. Section 3, following and slightly extending results from (Achatz et al., 2010), considers the the WKB theory of short wavelength internal wave packets, including equations for their amplification at high altitudes, and it discusses the validity of the said sound-proof models as a function of the background potential temperature stratification. Section 4 summarizes our main conclusions.

2 Sound-proof models in their design regime

2.1 Model equations

Ignoring coriolis effects and non-resolved-scale closures, the compressible, pseudo-incompressible, and the Lipps & Hemler anelastic model equations – suitably non-dimensionalized – read,

Compressible Euler equations

$$\begin{aligned} \rho_t + \nabla\cdot(\rho\mathbf{v}) &= 0 && (6a)\\ (\rho\mathbf{v})_t + \nabla\cdot(\rho\mathbf{v}\circ\mathbf{v}) + P\nabla\pi &= -\rho\mathbf{k} && (6b)\\ P_t + \nabla\cdot(P\mathbf{v}) &= 0 && (6c) \end{aligned}$$

Pseudo-incompressible model

$$\begin{aligned} \rho_t + \nabla\cdot(\rho\mathbf{v}) &= 0 && (7a)\\ (\rho\mathbf{v})_t + \nabla\cdot(\rho\mathbf{v}\circ\mathbf{v}) + \overline{P}\nabla\pi &= -\rho\mathbf{k} && (7b)\\ \nabla\cdot(\overline{P}\mathbf{v}) &= 0 && (7c) \end{aligned}$$

Lipps & Hemler anelastic model

$$\begin{aligned} \nabla\cdot(\overline{\rho}\mathbf{v}) &= 0 && (8a)\\ (\overline{\rho}\mathbf{v})_t + \nabla\cdot(\overline{\rho}\mathbf{v}\circ\mathbf{v}) + \overline{\rho}\nabla\widehat{\pi} &= \overline{\rho}\,\frac{\theta-\overline{\theta}}{\overline{\theta}}\,\mathbf{k} && (8b)\\ (\overline{\rho}\theta)_t + \nabla\cdot(\overline{\rho}\theta\mathbf{v}) &= 0 && (8c) \end{aligned}$$

Here $(\rho,\mathbf{v})$ are the density and flow velocity, $P = p^{1/\gamma} = \rho\theta$ is a modified thermodynamic pressure variable, θ the potential temperature, and $\pi = p^{\kappa}/\kappa$ where $\kappa = (\gamma-1)/\gamma$, and $\gamma = c_p/c_v$ is the ratio of the specific heat capacities. In the pseudo-incompressible model from (7), the thermodynamic pressure field is considered fixed and varying in the vertical only, so that $P \equiv \overline{P}(z)$. In contrast, for the anelastic model in (8) the density is frozen in time and prescribed as a function of the vertical only, so that $\rho \equiv \overline{\rho}(z)$.

As regards the chosen non-dimensionalization, let an asterisc denote dimensional variables. Then the dimensionless quantities appearing in (6) are defined as

$$t = \frac{t^* c_{\rm ref}}{h_{\rm sc}}, \qquad \mathbf{x} = \frac{\mathbf{x}^*}{h_{\rm sc}}, \qquad \rho = \frac{\rho^*}{\rho_{\rm ref}}, \qquad p = \frac{p^*}{p_{\rm ref}}, \qquad \mathbf{v} = \frac{\mathbf{v}^*}{c_{\rm ref}}, \qquad \rho\theta = p^{1/\gamma}, \tag{9}$$

where $c_{\rm ref} = \sqrt{p_{\rm ref}/\rho_{\rm ref}}$ and $h_{\rm sc} = p_{\rm ref}/\rho_{\rm ref}\,g$, and where $p_{\rm ref}, \rho_{\rm ref}$, and g denote the sea-level pressure, the corresponding density at a temperature of 300 K, say, and the acceleration of gravity, respectively.

In all three cases, $\overline{\theta}(z)$ is the mean background potential temperature distribution which defines the background pressure variable, $\overline{P}(z)$, and the background density, $\overline{\rho}(z)$, via $d\overline{p}/dz = -\overline{\rho}\,g$, $\overline{p}(0) = 1$, $\overline{\rho}\,\overline{\theta} = \overline{P}$, and $\overline{P} \equiv \overline{p}^{1/\gamma}$. For later reference we note the exact solution,

$$\overline{p}(z) = \overline{P}(z)^{\gamma} = \left[\kappa\overline{\pi}(z)\right]^{\frac{1}{\kappa}}, \quad \overline{\rho}(z) = \overline{P}(z)/\overline{\theta}(z), \quad \text{where} \quad \overline{\pi}(z) = \frac{1}{\kappa} - \int_0^z \frac{1}{\overline{\theta}(\zeta)}\,d\zeta\,. \tag{10}$$

We also note that in the anelastic model (8) the pressure-related quantity $\widehat{\pi}$ is defined as

$$\widehat{\pi} = \frac{p-\overline{p}}{\overline{\rho}}, \tag{11}$$

i.e., it is a density-scaled perturbation of the pressure, p, but not of the Exner pressure, π.

2.2 Scaled variables

The subsequent scale analysis is facilitated by rewriting (6) in a non-conservative (advective) perturbational form with the primary unknowns

$$\theta' = \theta - \overline{\theta}(z)\,, \qquad \mathbf{v}\,, \qquad \pi' = \pi - \overline{\pi}(z)\,. \tag{12}$$

The hydrostatic background variables satisfy

$$d\overline{\pi}/dz = 1/\overline{\theta} \qquad \text{with} \qquad \overline{\pi}(0) = 1/\kappa\,. \tag{13}$$

This yields the equivalent advective form of the compressible Euler equations

$$\theta'_t + \mathbf{v}\cdot\nabla\theta' + w\,\frac{d\overline{\theta}}{dz} = 0 \tag{14a}$$

$$\mathbf{v}_t + \mathbf{v}\cdot\nabla\mathbf{v} + (\overline{\theta}+\theta')\nabla\pi' = \frac{\theta'}{\overline{\theta}}\,\mathbf{k} \tag{14b}$$

$$\pi'_t + \mathbf{v}\cdot\nabla\pi' + w\frac{d\overline{\pi}}{dz} + \gamma\kappa(\overline{\pi}+\pi')\nabla\cdot\mathbf{v} = 0 \tag{14c}$$

A further transformation of variables reveals the asymptotic scalings in terms of the Mach number, ε. We nondimensionalize time by a characteristic advection time scale, so that

$$\tau = \varepsilon\, t \tag{15}$$

and let

$$\theta(t,\mathbf{x},z;\varepsilon) = 1 + \varepsilon^{\mu}\,\overline{\Theta}(z) + \varepsilon^{\mu+\nu}\,\widetilde{\theta}(\tau,\mathbf{x},z;\varepsilon) \qquad (\nu = 1-\mu/2) \tag{16a}$$

$$\pi(t,\mathbf{x},z;\varepsilon) = \overline{\pi}(z) + \varepsilon\,\widetilde{\pi}(\tau,\mathbf{x},z;\varepsilon) \tag{16b}$$

$$\mathbf{v}(t,\mathbf{x},z;\varepsilon) = \varepsilon\,\widetilde{\mathbf{v}}(\tau,\mathbf{x},z;\varepsilon) \tag{16c}$$

The velocity, $\mathbf{v}$, was nondimensionalized by $\sqrt{p_{\rm ref}/\rho_{\rm ref}}$, which is comparable to the sound speed; whereupon the scaling in (16c) implies low Mach number flow when $\varepsilon \ll 1$. The representation of the background potential temperature stratification,

$$\overline{\theta}(z) = 1 + \varepsilon^{\mu}\,\overline{\Theta}(z)\,, \tag{17}$$

follows from the stratification regime in (3). The exponent ν determines the scaling of the dynamic potential temperature perturbations. Its specific value as given in (16a) implies the correct scaling for internal gravity waves as we will see shortly. Furthermore, $\overline{\pi}(z)$ denotes the background Exner pressure distribution given the stratification from (3). We assume a pressure perturbation amplitude of the order of the Mach number, $O(\varepsilon)$, so as to not preclude leading-order acoustic modes at this stage.

For compressible flows, the new variables $\widetilde{\theta},\widetilde{\pi},\widetilde{\mathbf{v}}$ satisfy

$$\widetilde{\theta}_\tau + \frac{1}{\varepsilon^{\nu}}\,\widetilde{w}\,\frac{d\overline{\Theta}}{dz} = -\widetilde{\mathbf{v}}\cdot\nabla\widetilde{\theta} \tag{18a}$$

$$\widetilde{\mathbf{v}}_\tau - \frac{1}{\varepsilon^{\nu}}\,\frac{\widetilde{\theta}}{\overline{\theta}}\,\mathbf{k} + \frac{1}{\varepsilon}\,(1+\varepsilon^{\mu}\overline{\Theta})\nabla\widetilde{\pi} = -\widetilde{\mathbf{v}}\cdot\nabla\widetilde{\mathbf{v}} - \varepsilon^{1-\nu}\widetilde{\theta}\nabla\widetilde{\pi} \tag{18b}$$

$$\widetilde{\pi}_\tau + \frac{1}{\varepsilon}\left(\gamma\kappa\overline{\pi}\nabla\cdot\widetilde{\mathbf{v}} + \widetilde{w}\frac{d\overline{\pi}}{dz}\right) = -\widetilde{\mathbf{v}}\cdot\nabla\widetilde{\pi} - \gamma\kappa\widetilde{\pi}\nabla\cdot\widetilde{\mathbf{v}} \tag{18c}$$

These equations are obtained from a straightforward *equivalent* transformation of the compressible flow equations in (6) without any asymptotic simplifications.

Table 2: Switching parameters in eqn. (19).

model	A	B	C
compressible	1	1	0
pseudo-incompressible	0	1	0
anelastic	0	0	1

Besides the tendencies of temporal change, there are three groups of terms in (18): the terms multiplied by $\varepsilon^{-\nu}$ induce internal waves, the terms multiplied by ε^{-1} represent the acoustic modes, and the terms on the right hand side cover all nonlinearities. In fact, all terms on the left hand sides are linear in the unknowns. Notice that all terms on the right are non-singular as $\varepsilon \to 0$, i.e., they are $O(\varepsilon^{\alpha})$ with $\alpha \geq 0$. This clean Mach number scaling of acoustic, internal wave, and nonlinear (advective) terms justifies in hindsight the choice $\nu = 1 - \mu/2$ introduced earlier.

2.3 Internal gravity waves

2.3.1 Gravity wave scaling

The compressible flow equations from (18) feature three distinct time scales for sound propagation, $\tau = O(\varepsilon)$, for internal waves, $\tau = O(\varepsilon^{\nu})$, and for advection, $\tau = O(1)$. In this section we consider solutions that do not feature sound waves but evolve on time scales comparable to the internal wave time scale. The only "sound-term" of order $O(\varepsilon^{-1})$ in the momentum equation is the one involving the pressure gradient. This term will reduce to order $O(\varepsilon^{-\nu})$, and thus induce changes on the internal wave time scale only, provided that the pressure perturbations satisfy $\widetilde{\pi} = \varepsilon^{1-\nu}\pi^*$ with $\pi^* = O(1)$. By introducing this additional rescaling of the pressure fluctuations and by adopting an internal wave time coordinate $\vartheta = \varepsilon^{-\nu}\tau$, the compressible, pseudo-incompressible, and anelastic systems can be represented as

$$\widetilde{\theta}_{\vartheta} + \widetilde{w}\,\frac{d\overline{\Theta}}{dz} = -\varepsilon^{\nu}\,\widetilde{\mathbf{v}}\cdot\nabla\widetilde{\theta} \tag{19a}$$

$$\widetilde{\mathbf{v}}_{\vartheta} - \frac{\widetilde{\theta}}{\overline{\theta}}\,\mathbf{k} + (1 + B\,\varepsilon^{\mu}\,\overline{\Theta})\nabla\pi^* = -\varepsilon^{\nu}\,\widetilde{\mathbf{v}}\cdot\nabla\widetilde{\mathbf{v}} - B\,\varepsilon^{\mu+\nu}\,\widetilde{\theta}\nabla\pi^* \tag{19b}$$

$$A\varepsilon^{\mu}\pi^*_{\vartheta} - C\varepsilon^{\mu}\,\frac{\gamma\kappa\overline{\pi}}{\overline{\theta}}\,\widetilde{w}\frac{d\overline{\Theta}}{dz} + \left(\gamma\kappa\overline{\pi}\nabla\cdot\widetilde{\mathbf{v}} + \widetilde{w}\frac{d\overline{\pi}}{dz}\right) = -A\varepsilon^{\mu+\nu}\,(\widetilde{\mathbf{v}}\cdot\nabla\pi^* + \gamma\kappa\pi^*\nabla\cdot\widetilde{\mathbf{v}}) \tag{19c}$$

with the choices of the switching parameters as summarized in Table 2.

We observe that in the gravity wave scaling all differences between the compressible model on the one hand and both of the sound-proof models on the other hand are of order $O(\varepsilon^{\mu})$ or smaller, i.e., at least of the order of the stratification strength. At leading order in ε, all models agree from a formal scaling perspective. Differences arise, formally, at $O(\varepsilon^{\mu})$ on the internal wave time scale with $\vartheta = O(1)$.

2.3.2 Regime of validity for the background stratification

The leading perturbation terms in (19) involve terms of order $O(\varepsilon^{\mu})$ in the linearized part on the left, and terms of order $O(\varepsilon^{\nu})$ in the nonlinear part of the equations on the right. This suggests that for $\mu < \nu$, i.e., for $\varepsilon^{\mu} \gg \varepsilon^{\nu}$, the linearized internal wave eigenmodes and eigenvalues of the three systems differ by $O(\varepsilon^{\mu})$ only, and the nonlinearities represent even higher-order effects. In this setting, we may

expect solutions of the three models that start from comparable internal wave initial data to remain close with differences of order $O(\varepsilon^\mu)$ over the internal wave time scale with $\vartheta = O(1)$. Yet, we are really interested in flow evolutions over advective time scales with $\tau = \varepsilon^\nu \vartheta = O(1)$. Over such longer time scales, the expected differences in the internal wave eigenfrequencies of order $O(\varepsilon^\mu)$ will accumulate to phase shifts of order $\varepsilon^\mu \cdot \vartheta = O(\tau \cdot \varepsilon^{\mu-\nu}) = O(\varepsilon^{\mu-\nu})$. As a consequence, the linearized internal wave solutions of the three models should remain asymptotically close even over advective time scales provided

$$\varepsilon^{\mu-\nu} = \varepsilon^{\frac{3}{2}\mu-1} = o(1) \qquad \text{as} \qquad \varepsilon \to 0 \qquad \text{or} \qquad \mu > \frac{2}{3}. \tag{20}$$

For any stratifications weaker than $d\overline{\theta}/dz = O(\varepsilon^{2/3})$, the internal wave dynamics of the compressible, pseudo-incompressible, and anelastic models should remain asymptotically close in terms of the flow Mach number *over advective time scales*. This is a considerable improvement over the original Ogura & Phillips' condition for the validity of their anelastic model which requires that $d\overline{\theta}/dz = O(\varepsilon^2)$. For $\varepsilon \sim 1/30$ the Ogura & Phillips' estimate amounts to potential temperature variations of the order of $\Delta\theta|_0^{h_{\rm sc}} \sim 0.33$ K over the pressure scale height, whereas our new estimate implies validity of the sound-proof models even if

$$\Delta\theta|_0^{h_{\rm sc}} \sim \theta_{\rm ref} h_{\rm sc} \cdot \frac{1}{\theta^*}\frac{d\theta^*}{dz^*} = T_{\rm ref}\,\frac{1}{\theta}\frac{d\theta}{dz} \sim 300\ {\rm K} \cdot (1/30)^{2/3} \sim 30\ {\rm K}, \tag{21}$$

where the asterisc denotes dimensional quantities.

Since all three models feature the same leading nonlinearities, we expect asymptotic agreement of the solutions over advective time scales as long as the fast linearized dynamics do not already lead to leading-order deviations between the model results, i.e., as long as $\mu > 2/3$.

2.3.3 Vertical mode decomposition and Sturm-Liouville eigenvalue problem

Assuming rigid-wall top and bottom boundaries at $z = 0$ and $z = H = O(1)$, respectively, and seeking horizontally travelling waves

$$\left(\widetilde{\theta}, \widetilde{\mathbf{u}}, \widetilde{w}, \pi^*\right)(\vartheta, \mathbf{x}, z) = \left(\check{\theta}, \check{\mathbf{u}}, \check{w}, \check{\pi}\right)(z)\ \exp\left(i\left[\omega\vartheta - \boldsymbol{\lambda}\cdot\mathbf{x}\right]\right), \tag{22}$$

the linearized version of (19) yields, after elimination of $\check{\theta}, \check{\mathbf{u}}$, and $\check{\pi}$ a Sturm-Liouville-type equation for a scaled vertical velocity structure function $W(z)$,

$$-\frac{d}{dz}\left(\frac{1}{\lambda^2 - A\,\varepsilon^\mu/\Lambda\overline{c}^2}\ \phi_{BC}\ \frac{dW}{dz}\right) + \phi_{BC}\ W = \Lambda\ (N^2\phi_{BC})\ W \tag{23}$$

with boundary conditions

$$W(0) = W(H) = 0. \tag{24}$$

Here we have used the following abbreviations

$$\phi_{BC} = \frac{\overline{\theta}^C}{\overline{\theta}^B\overline{P}}, \quad \overline{c}^2 = \frac{\gamma\overline{p}}{\overline{\rho}}, \quad N^2 = \frac{1}{\overline{\theta}}\frac{d\overline{\Theta}}{dz}, \tag{25}$$

and

$$\Lambda = \frac{1}{\omega^2}, \qquad W = \begin{cases} \overline{P}\check{w} & \text{compressible or pseudo-incompressible} \\ \overline{\rho}\check{w} & \text{anelastic} \end{cases}. \tag{26}$$

Here $\overline{\theta}^B$ and $\overline{\theta}^C$ are to be read as "$\overline{\theta}$ to the power B and C", respectively. (Notice that there is a typographical error in (Klein et al., 2010) in the first equation of (25).)

For $A = 0$, i.e., for either the anelastic or the pseudo-incompressible model, and for any fixed horizontal wave number vector, λ, eqs. (23), (24) represent a classical Sturm-Liouville eigenvalue problem with the following two key features: (i) There is a sequence of eigenvalues and associated eigenfunctions, $(\Lambda_k^0, W_k^0)_{k=0}^{\infty}$ satisfying $0 < \Lambda_0^0 < \Lambda_1^0 \ldots$, and $\Lambda_k^0 \to \infty$ as $k \to \infty$. Here $k = 0$ represents the leading, vertically non-oscillatory mode, and the eigenmodes oscillate more strongly with higher k, and (ii) the $(W_k^0)_{k=0}^{\infty}$ form an orthonormal basis of a Hilbert space of functions $f : [0,H] \mapsto I\!R$ with scalar product $\langle U,V \rangle = \int_0^H U\ (N^2 \phi_{BC})\ V\ dz$.

We conclude that the two sound-proof models considered here feature well-defined internal wave modes, one such hierarchy of eigenvalues and vertical structures for each wave number vector, λ. The only differences in the linearized eigenmodes between the pseudo-incompressible and the present anelastic model consist of the scaling factor of $\overline{\theta} = \overline{P}/\overline{\rho}$ in the definition of the structure function $W(z)$ in (26), and of the slightly different way in which the background potential temperature distribution enters the Sturm-Liouville equation according to (25). The compressible and pseudo-incompressible models share the definition of both W and ϕ_{BC}.

As regards the eigenvalues and eigenfunctions for the compressible case, one must distinguish, going back to (23), the cases $\varepsilon^\mu / \Lambda \overline{c}^2 \ll 1$ and $\varepsilon^\mu / \Lambda \overline{c}^2 \geq O(1)$. The former corresponds to internal waves of the compressible system, whereas the latter represents acoustic modes. For the internal wave modes, two of the authors of (Klein et al., 2010) proved rigorously that the difference between the eigenvalues and eigenfunctions of the compressible, anelastic, and pseudo-incompressible systems are of the order $O(\varepsilon^\mu)$ as $\varepsilon \to 0$. The proof takes advantage of the fact that the eigensolutions depend smoothly on the parameters of a regular Sturm-Liouville problem. This corroborates the analysis on the regime of validity of the sound-proof models w.r.t. the background potential temperature stratification in section 22.32.3.2.

Klein et al. (2010) provide a few explicit computational examples of eigenmodes and eigenfunctions spanning a range of horizontal wavenumbers and vertical mode numbers that roughly cover the design regime with characteristic length scale $L \sim h_{\rm sc}$. Across the board they find surprisingly good agreement of relative deviations between the sound-proof and compressible results. Given values of $\varepsilon^\mu \sim 0.1$, the relative errors in the eigenvalues were generally $O(10e^{-3})$ and less.

2.3.4 The long-wave limit

Equation (23), at a first glance, suggests that compressibility may play less of a subordinate role for large-scale internal gravity waves with $|\lambda| \ll 1$ as in this case the two terms in the denominator of the first term, $\lambda^2 - \varepsilon^\mu / \Lambda \overline{c}^2$, could become comparable. Multiplying (23) by λ^2 one obtains a rescaled eigenvalue problem for $\Lambda^*(\lambda) = \lambda^2 \Lambda$,

$$-\frac{d}{dz}\left(\frac{1}{1-\varepsilon^\mu/\Lambda^*(\lambda)\overline{c}^2}\ \phi\ \frac{dW}{dz}\right) + \lambda^2\ \phi\ W = \Lambda^*(\lambda)\ (N^2\phi)\ W\,. \tag{27}$$

As $\lambda^2 \to 0$, the equation approaches a well-defined limit in which the second term on the left vanishes asymptotically, and the term $\varepsilon^\mu / \Lambda^* \overline{c}^2$ remains a small perturbation in the denominator of the second-derivative term. As a consequence,

$$\lambda^2 \Lambda_k \to \Lambda_k^*(0) \qquad \text{as} \qquad |\lambda| \to 0\,, \tag{28}$$

where $\Lambda_k^*(0)$ is an eigenvalue of the limit problem,

$$-\frac{d}{dz}\left(\frac{1}{1-\varepsilon^\mu/\Lambda^*(\lambda)\overline{c}^2}\ \phi\ \frac{dW}{dz}\right) = \Lambda^*(\lambda)\ (N^2\phi)\ W \tag{29}$$

with the same rigid-wall boundary conditions. To capture the behavior of internal waves at large horizontal scales, Coriolis effects must be accounted for in addition in the future.

3 Nonlinear WKB theory for internal wave packets

Here we recall recent work by Achatz et al. (2010) who study internal gravity wave packets with amplitudes near the threshold of wave breaking and wavelengths, ℓ, satisfying

$$kh_{\rm sc} = \frac{2\pi}{\ell} h_{\rm sc} = O(\delta^{-1}) \qquad \text{as} \qquad (\delta \to 0)\,. \tag{30}$$

These authors perform a WKB analysis showing that the compressible Euler and pseudo-incompressible models have the exact same leading-order asymptotics in the considered regime, whereas results from the Lipps and Hemler anelastic model are argued, without explicit calculations being shown, to differ in terms of the leading nonlinear effects concerning the wave-mean flow interaction and the generation of higher harmonic WKB modes.

Here we repeat the main steps of their analysis but focus on the difference between the anelastic and pseudo-incompressible models. The compressible Euler equations need not be considered anymore, as up to the order considered, their asymptotics is equivalent to that of the pseudo-incompressible model.

We start by reiterating the scalings of the flow variables considered in (Achatz et al., 2010). The velocity amplitudes associated with the near-breaking regime are estimated by requiring that over the characteristic internal wave oscillation time, represented by the Brunt-Väisälä frequency, $T_{\rm int} \sim 2\pi N^{-1}$ where $N = \sqrt{g/\overline{\theta}\; d\overline{\theta}/dz}$, particles get displaced by distances comparable to the typical wavelength in the wave packet. Thus, if $w_{\rm ref}$ denotes a characteristic vertical perturbation flow velocity, one has

$$\frac{2\pi w_{\rm ref}}{N} \sim \ell = 2\pi\delta h_{\rm sc} \qquad \text{or} \qquad w_{\rm ref} \sim \delta N h_{\rm sc} \qquad \text{for some} \qquad \delta \ll 1. \tag{31}$$

For the flow Mach number this implies

$$\varepsilon^2 = \frac{w_{\rm ref}^2}{c_{\rm ref}^2} \sim \delta^2 \frac{N^2 h_{\rm sc}^2}{c_{\rm ref}^2} = \delta^2 \left(\frac{g h_{\rm sc}}{c_{\rm ref}^2}\right)\left(\frac{h_{\rm sc}}{\overline{\theta}}\frac{d\overline{\theta}}{dz}\right). \tag{32}$$

Noticing that the (compressible) background hydrostatic balance implies $gh_{\rm sc} = p_{\rm ref}/\rho_{\rm ref} = c_{\rm ref}^2$ and allowing for leading order stratification so that the last factor on the right is of order unity, one arrives at a distinguished limit between the flow Mach number and the dimensionless characteristic wavelength,

$$\frac{w_{\rm ref}}{c_{\rm ref}} \sim \varepsilon \sim \delta \sim \frac{\ell}{2\pi h_{\rm sc}}. \tag{33}$$

Using the standard polarization conditions for planar internal gravity waves one finds the appropriate perturbation scalings for the Exner pressure and potential temperature,

$$\pi' = \frac{\pi - \overline{\pi}}{\overline{\pi}} = O(\varepsilon^2), \qquad \theta' = \frac{\theta - \overline{\theta}}{\overline{\theta}} = O(\varepsilon). \tag{34}$$

For the dimensionless variables

$$\hat{x} = \frac{x}{\ell}, \quad \hat{z} = \frac{z}{\ell}, \quad \hat{t} = \frac{t\, w_{\rm ref}}{\ell}, \quad \hat{u} = \frac{u}{w_{\rm ref}}, \quad \hat{w} = \frac{w}{w_{\rm ref}}, \quad \hat{\pi} = \frac{\pi}{\overline{\pi}(0)}, \quad \hat{\theta} = \frac{\theta}{T_{\rm ref}}, \tag{35}$$

the compressible Euler equations then read

$$\varepsilon^2 \frac{D\hat{u}}{D\hat{t}} + \frac{\hat{\theta}}{\kappa}\frac{\partial \hat{\pi}}{\partial \hat{x}} = 0, \tag{36a}$$

$$\varepsilon^2 \frac{D\hat{w}}{D\hat{t}} + \frac{\hat{\theta}}{\kappa}\frac{\partial \hat{\pi}}{\partial \hat{z}} = -\varepsilon, \tag{36b}$$

$$\frac{D\hat{\theta}}{D\hat{t}} = 0, \tag{36c}$$

$$\frac{D\hat{\pi}}{D\hat{t}} + \frac{\kappa}{1-\kappa}\hat{\pi}\hat{\nabla}\cdot\vec{\hat{v}} = 0, \tag{36d}$$

where $D/D\hat{t}$ is the Lagrangian time derivative, and $\kappa = (\gamma-1)/\gamma$ as before (see discussion following (8)). Note that $\hat{x},\hat{z}$, and $\hat{t}$ resolve the small space and short time scales associated with the local internal wave description within a wave packet. In contrast,

$$(\tau,\chi,\zeta) = \varepsilon(\hat{t},\hat{x},\hat{z}) \tag{37}$$

resolve the large scales comparable with the pressure scale height $h_{\rm sc}$ and the associated advection time scale based on $w_{\rm ref}$. Note also that Achatz et al. (2010) do not assume weak potential temperature background stratification, so that the potential temperature scale height satisfies $H_\theta = \mathscr{O}(h_{\rm sc})$ as $\varepsilon \to 0$ asymptotically, although in practice the factor of proportionality may be as large as $H_\theta/h_{\rm sc} \sim 5...7$.

In line with the perturbation order estimates in (34), one next introduces

$$\hat{u} = \tilde{u}\,, \qquad \hat{w} = \tilde{w}\,, \qquad \hat{\theta} = \overline{\theta} + \varepsilon\tilde{\theta}\,, \qquad \hat{\pi} = \kappa\,(\overline{\pi} + \varepsilon^2\tilde{\pi})\,, \tag{38}$$

assuming that $\overline{\theta},\overline{\pi}$ depend on $\zeta = \varepsilon\hat{z}$ only and satisfy leading-order hydrostatic balance,

$$\frac{d\overline{\pi}}{d\zeta} = -\frac{1}{\overline{\theta}}\,, \qquad \overline{\pi}(0) = \frac{1}{\kappa}\,. \tag{39}$$

The compressible Euler, pseudo-incompressible and anelastic models may now be cast in a common form in terms of $(\tilde{u},\tilde{w},\tilde{\theta},\tilde{\pi})$,

$$\frac{\partial\tilde{u}}{\partial\hat{t}} + \overline{X}\frac{\partial\tilde{\pi}}{\partial\hat{x}} = -\left\{\tilde{u}\frac{\partial\tilde{u}}{\partial\hat{x}} + \tilde{w}\frac{\partial\tilde{u}}{\partial\hat{z}} + \varepsilon\tilde{X}\frac{\partial\tilde{\pi}}{\partial\hat{x}}\right\}, \tag{40a}$$

$$\frac{\partial\tilde{w}}{\partial\hat{t}} + \overline{X}\frac{\partial\tilde{\pi}}{\partial\hat{z}} - \frac{\tilde{\theta}}{\overline{\theta}} = -\left\{\tilde{u}\frac{\partial\tilde{w}}{\partial\hat{x}} + \tilde{w}\frac{\partial\tilde{w}}{\partial\hat{z}} + \varepsilon\tilde{X}\frac{\partial\tilde{\pi}}{\partial\hat{z}}\right\}, \tag{40b}$$

$$\frac{\partial\tilde{\theta}}{\partial\hat{t}} + \tilde{w}\frac{d\overline{\theta}}{d\zeta} = -\left\{\tilde{u}\frac{\partial\tilde{\theta}}{\partial\hat{x}} + \tilde{w}\frac{\partial\tilde{\theta}}{\partial\hat{z}}\right\}, \tag{40c}$$

$$\mathrm{div}(\overline{R}\tilde{\mathbf{v}}) = -\varepsilon^2\tilde{C}\,, \tag{40d}$$

where

$$\frac{D}{D\hat{t}} = \frac{\partial}{\partial\hat{t}} + \tilde{u}\frac{\partial}{\partial\hat{x}} + \tilde{w}\frac{\partial}{\partial\hat{z}} \qquad \text{and} \qquad \mathrm{div}(\tilde{\mathbf{v}}) = \left(\frac{\partial\tilde{u}}{\partial\hat{x}} + \frac{\partial\tilde{w}}{\partial\hat{z}}\right). \tag{41}$$

The three models emerge under the following choices

compressible Euler

$$\overline{X} = \overline{\theta}\,, \quad \tilde{X} = \tilde{\theta}\,, \quad \overline{R} = \overline{P}\,, \quad \tilde{C} = \frac{1-\kappa}{\kappa}\frac{\overline{P}}{\overline{\pi}}\left\{\frac{D\tilde{\pi}}{D\hat{t}} - \frac{\kappa}{1-\kappa}\tilde{\pi}\,\mathrm{div}(\tilde{\mathbf{v}})\right\}, \tag{42a}$$

pseudo-incompressible

$$\overline{X} = \overline{\theta}\,, \quad \tilde{X} = \tilde{\theta}\,, \quad \overline{R} = \overline{P}\,, \quad \tilde{C} = 0\,, \tag{42b}$$

anelastic

$$\overline{X} = 1\,, \quad \tilde{X} = 0\,, \quad \overline{R} = \overline{\rho}\,, \quad \tilde{C} = 0\,. \tag{42c}$$

where $\overline{\rho}$ and $\overline{P}$ are defined through

$$\overline{\rho}\,\overline{\theta} = \overline{P} = (\kappa\overline{\pi})^{\frac{1-\kappa}{\kappa}}\,. \tag{43}$$

As Achatz et al. (2010) have shown that the subsequent WKB theory leads to identical leading and first order results for the compressible and pseudo-incompressible models, we compare only the pseudo-incompressible and anelastic models below.

Consider the general large amplitude WKB solution ansatz for solutions of (40)

$$\begin{pmatrix} \tilde{u} \\ \tilde{w} \\ \tilde{\theta} \\ \tilde{\pi} \end{pmatrix} = \begin{pmatrix} U_0^{(0)} \\ W_0^{(0)} \\ \Theta_0^{(1)} \\ \Pi_0^{(2)} \end{pmatrix} (\tau,\chi,\zeta) + \Re \left[\begin{pmatrix} U_1^{(0)} \\ W_1^{(0)} \\ \Theta_1^{(1)} \\ \Pi_1^{(2)} \end{pmatrix} (\tau,\chi,\zeta) \exp\left(i \frac{\varphi(\tau,\chi,\zeta)}{\varepsilon} \right) \right]$$
$$+ \varepsilon \left[\begin{pmatrix} U_0^{(1)} \\ W_0^{(1)} \\ \Theta_0^{(2)} \\ \Pi_0^{(3)} \end{pmatrix} (\tau,\chi,\zeta) + \Re \sum_{\alpha=1}^{\infty} \begin{pmatrix} U_\alpha^{(1)} \\ W_\alpha^{(1)} \\ \Theta_\alpha^{(2)} \\ \Pi_\alpha^{(3)} \end{pmatrix} (\tau,\chi,\zeta) \exp\left(i\alpha \frac{\varphi(\tau,\chi,\zeta)}{\varepsilon} \right) \right] + o(\varepsilon), \tag{44}$$

with $(\tau,\chi,\zeta) = \varepsilon(\hat{t},\hat{x},\hat{z})$ defined in (37), and $\Re$ denoting the real part of a complex number. The label "large amplitude" is justified because we do not assume small $\tilde{u},\tilde{w}$ so that the advection terms on the right of (37) are formally of order unity.

3.1 Leading-order analysis

Applying standard WKB procedures to the divergence constraint in (40d) one finds from the terms proportional to $\exp(i\varphi/\varepsilon)$ the small scale solenoidality constraint

$$i\left(\frac{\partial\varphi}{\partial\chi} U_1^{(0)} + \frac{\partial\varphi}{\partial\zeta} W_1^{(0)} \right) = 0. \tag{45}$$

This condition reduces the advection terms, which formally appear at leading order as mentioned above, to at most order $\mathcal{O}(\varepsilon)$.

The mean-flow contributions (zero power in $\exp(i\varphi/\varepsilon)$) of the vertical momentum and entropy equations in (40b) and (40c) then yield, respectively,

$$\Theta_0^{(1)} = W_0^{(0)} = 0. \tag{46}$$

Using these results in (36a) – (36d) we find

$$\underbrace{\begin{pmatrix} -i\hat{\omega} & 0 & 0 & ik \\ 0 & -i\hat{\omega} & -N & im \\ 0 & N & -i\hat{\omega} & 0 \\ ik & im & 0 & 0 \end{pmatrix}}_{M(\hat{\omega},k,m)} \begin{pmatrix} U_1^{(0)} \\ W_1^{(0)} \\ \Theta_1^{(1)} \\ \overline{N}\overline{\theta} \\ \overline{X}\Pi_1^{(2)} \end{pmatrix} = 0 \tag{47}$$

where

$$\hat{\omega} = \omega - kU_0^{(0)}, \qquad \omega = -\frac{\partial\varphi}{\partial\tau}, \qquad k = \frac{\partial\varphi}{\partial\chi}, \qquad m = \frac{\partial\varphi}{\partial\zeta}. \tag{48}$$

These are the linearized internal plane wave equations from Boussinesq theory, which is expected, because variations of the background density over the characteristic wavelength of the considered wave packets are $\mathcal{O}(\varepsilon)$ only.

To allow for nontrivial solutions, the matrix M in (47) must be singular and this leads to the classical internal wave dispersion relation for the Boussinesq model,

$$\hat{\omega}^2(k,m) = N^2 \frac{k^2}{k^2+m^2}. \tag{49}$$

From the definitions in (48) one obtains (after some tedious calculations) the ray-tracing equations

$$\left(\frac{\partial}{\partial\tau}+\vec{c}_g\cdot\nabla_{(\chi,\zeta)}\right)(k,m,\omega)=\left(0,-k\frac{\partial U_0^{(0)}}{\partial\zeta},k\frac{\partial U_0^{(0)}}{\partial\tau}\right) \tag{50}$$

with the group velocity

$$\vec{c}_g=\left(U_0^{(0)}+\frac{\partial\hat{\omega}}{\partial k},\frac{\partial\hat{\omega}}{\partial m}\right). \tag{51}$$

Given the dispersion relation that renders M singular, the polarization relations determining relationships between the amplitudes $U_1^{(0)},W_1^{(0)},\Theta_1^{(1)}$, and $\Pi_1^{(2)}$ are obtained straightforwardly from the nullspace right eigenvector of M, see (Achatz et al., 2010),

$$\left(U_1^{(0)},\,W_1^{(0)},\,\frac{\Theta_1^{(1)}}{N\overline{\theta}},\,\overline{X}\Pi_1^{(2)}\right)^T=\left(-i\frac{m}{k}\frac{\hat{\omega}}{N},\,i\frac{\hat{\omega}}{N},\,1,\,-i\frac{m}{k^2}\frac{\hat{\omega}^2}{N}\right)^T\frac{\Theta_1^{(1)}}{N\overline{\theta}}. \tag{52}$$

It follows that at leading order the pseudo-incompressible and anelastic models both reproduce the plane wave equations from Boussinesq theory. The only difference is the pressure scaling by $\overline{X}$ which implies $\Pi_1^{(2)}\big|_{\text{anel.}}=\overline{\theta}\,\Pi_1^{(2)}\big|_{\text{psinc.}}$. Note that $\overline{\theta}$ depends on $\zeta=\varepsilon\hat{z}$ only, so that it is constant to leading order in ε across the present characteristic internal wavelength.

3.2 First-order analysis

3.2.1 First-order Fourier components

At first order the terms in the divergence constraint, (40d), proportional to $e^{2i\varphi/\varepsilon}$ yield

$$ikU_\alpha^{(1)}+imW_\alpha^{(1)}=0\qquad(\alpha>1). \tag{53}$$

Making use of this relation and the fact that the leading-order mean flow is horizontally homogeneous (see (64) below), we find from the terms proportional to $\exp(i\varphi/\varepsilon)$,

$$M(\hat{\omega},k,m)\begin{pmatrix}U_1^{(1)}\\W_1^{(1)}\\\dfrac{\Theta_1^{(2)}}{N\overline{\theta}}\\\overline{X}\Pi_1^{(3)}\end{pmatrix}=-Q, \tag{54a}$$

where

$$Q=\begin{pmatrix}\dfrac{\partial U_1^{(0)}}{\partial\tau}+U_0^{(0)}\dfrac{\partial U_1^{(0)}}{\partial\chi}+W_1^{(0)}\dfrac{\partial U_0^{(0)}}{\partial\zeta}+\overline{X}\dfrac{\partial\Pi_1^{(2)}}{\partial\chi}+\left(ikU_0^{(1)}+imW_0^{(1)}\right)U_1^{(0)}\\[2ex]\dfrac{\partial W_1^{(0)}}{\partial\tau}+U_0^{(0)}\dfrac{\partial W_1^{(0)}}{\partial\chi}+\overline{X}\dfrac{\partial\Pi_1^{(2)}}{\partial\zeta}+\left(ikU_0^{(1)}+imW_0^{(1)}\right)W_1^{(0)}\\[2ex]\dfrac{\partial}{\partial\tau}\left(\dfrac{\Theta_1^{(1)}}{N\overline{\theta}}\right)+U_0^{(0)}\dfrac{\partial}{\partial\chi}\left(\dfrac{\Theta_1^{(1)}}{N\overline{\theta}}\right)+\left(ikU_0^{(1)}+imW_0^{(1)}\right)\dfrac{\Theta_1^{(1)}}{N\overline{\theta}}\\[2ex]\dfrac{\partial U_1^{(0)}}{\partial\chi}+\dfrac{\partial W_1^{(0)}}{\partial\zeta}+\dfrac{W_1^{(0)}}{\overline{R}}\dfrac{d\overline{R}}{d\zeta}\end{pmatrix}. \tag{54b}$$

Multiplying these equations from the left with the transpose complex conjugate of the null-space vector of the adjoint of $M(\hat{\omega},k,m)$, i.e., by

$$\left(U_1^{(0)},\,W_1^{(0)},\,\frac{\Theta_1^{(1)}}{N\overline{\theta}},\,\overline{X}\Pi_1^{(2)}\right)^*=\left(i\frac{m}{k}\frac{\hat{\omega}}{N},\,-i\frac{\hat{\omega}}{N},\,1,\,i\frac{m}{k^2}\frac{\hat{\omega}^2}{N}\right)\left[\frac{\Theta_1^{(1)}}{N\overline{\theta}}\right]^*, \tag{55}$$

one obtains from the real part of (54)[1]

$$\frac{\partial E'}{\partial \tau} + \nabla_{(\chi,\zeta)} \cdot \left(\vec{c}_g E' \right) = -\frac{\overline{R}/\overline{X}}{2} \, \Re \left(U_1^{(0)\,*} W_1^{(0)} \right) \frac{\partial U_0^{(0)}}{\partial \zeta} \tag{56}$$

where

$$E' = \frac{\overline{R}/\overline{X}}{4} \left(\left| U_1^{(0)} \right|^2 + \left| W_1^{(0)} \right|^2 + \left| \frac{\Theta_1^{(1)}}{N\overline{\theta}} \right|^2 \right) \equiv \frac{\overline{R}/\overline{X}}{2} \left| \frac{\Theta_1^{(1)}}{N\overline{\theta}} \right|^2 . \tag{57}$$

Using the polarization relations from (52) and the ray-tracing equations (50) one finally obtains the principle of wave-action conservation Bretherton (1966); Grimshaw (1975); Müller (1976)

$$\frac{\partial}{\partial \tau} \left(\frac{E'}{\hat{\omega}} \right) + \nabla_{(\chi,\zeta)} \cdot \left(\vec{c}_g \frac{E'}{\hat{\omega}} \right) = 0 . \tag{58}$$

Comparing with (42) we notice that

$$\overline{R}/\overline{X} = \begin{cases} \overline{P}/\overline{\theta} \equiv \overline{\rho} & \text{pseudo} - \text{incompressible} \\ \overline{\rho}/1 \equiv \overline{\rho} & \text{anelastic} \end{cases} \tag{59}$$

equals the background density for both the sound-proof models considered here. Since also the dispersion relation, (49), and the polarization conditions, (52), for the wave packets are the same, we conclude that *even for leading-order stratification* with $(1/\overline{\theta}) d\overline{\theta}/dz = \mathcal{O}(1)$ as $\varepsilon \to 0$, both models should produce the exact same amplification of wave amplitudes as a wave packet travels upwards to regions of low density.

3.2.2 Second-order Fourier components

The terms proportional to $\exp(i2\varphi/\varepsilon)$ now include nonlinear advection and pressure gradient terms terms, where the latter active yield one contribution each in the vertical momentum balance and in the potential temperature transport equation that are active only for the pseudo-incompressible model, viz.

$$M(2\hat{\omega}, 2k, 2m) \begin{pmatrix} U_2^{(1)} \\ W_2^{(1)} \\ \Theta_2^{(2)}/(N\overline{\theta}) \\ \overline{X}\Pi_2^{(3)} \end{pmatrix} = \begin{pmatrix} -D_1^{\overline{\rho}} U_1^{(0)} \\ -D_1^{\overline{\rho}} W_1^{(0)} - \frac{1}{2} \left(\frac{\tilde{X}_1^{(0)}}{\overline{\theta}} \right)^2 \\ -\frac{1}{N\overline{\theta}} D_1^{\overline{\rho}} \Theta_1^{(1)} + \frac{1}{2} \frac{\tilde{X}_1^{(0)}}{N\overline{\theta}} W_1^{(0)} N^2 \\ 0 \end{pmatrix} \tag{60}$$

where

$$D_1^{\overline{\rho}} = \frac{1}{2} \left(U_1^{(0)} \frac{\partial}{\partial \chi} + W_1^{(0)} \frac{\partial}{\partial \zeta} - \frac{1}{\overline{\rho}} \left(\frac{\overline{\rho} U_1^{(0)}}{\partial \chi} + \frac{\overline{\rho} W_1^{(0)}}{\partial \zeta} \right) \right) . \tag{61}$$

Note that $D_1^{\overline{\rho}}$ differs from D_1 in (Achatz et al., 2010) which features the equivalent of $\overline{P}$ instead of $\overline{\rho}$ in the divergence term.

We observe that $M(2\hat{\omega}, 2k, 2m)$ is *non-singular*, because $\hat{\omega}$, k, and m are already related by the dispersion relation in (49), and $\hat{\omega}(2k, 2m) \neq 2\,\hat{\omega}(k, m)$. As a consequence, the system can be solved for the unknowns $\left(U_2^{(1)},\, W_2^{(1)},\, \Theta_2^{(2)}/(N\overline{\theta}),\, \overline{X}\Pi_2^{(3)} \right)$, and no additional solvability constraint on the right-hand terms arises.

[1] The imaginary part yields a predictive equation for the large-scale and slow-time part of the wave phase $\beta = \arctan(\Im\Theta_1^{(1)}/\Re\Theta_1^{(1)})$ which, however, is not needed below.

The right-hand side of (60) involves the effects of nonlinear advection, which are identical for the anelastic and pseudo-incompressible models and captured through the terms involving $D_1^{\overline{\rho}}$. But, there are two effects which differ between the two models. The first difference results from the nonlinearity of the pressure term (last term in the second component on the right of (60)). The second difference arises in the potential temperature equation (last term in the third component of (60)), and it is due to the velocity field obeying different divergence constraints in the pseudo-incompressible and anelastic models. Since $\tilde{X} = \widetilde{\theta}$ for the pseudo-incompressible model, and $\tilde{X} \equiv 0$ for the anelastic one, the two terms are missing in the latter. Hence we expect to see differences between anelastic and pseudo-incompressible simulations in the second Fourier modes proportional to $\exp(i2\phi(\tau,\chi,\zeta)/\varepsilon)$.

3.2.3 Higher-order Fourier components

The higher-order terms proportional to $\exp(i\alpha\varphi/\varepsilon)$ for $\alpha > 2$ yield

$$M(\alpha\hat{\omega}, \alpha k, \alpha m) \left(U_\alpha^{(1)},\ W_\alpha^{(1)},\ \frac{\Theta_\alpha^{(2)}}{N\overline{\theta}},\ \overline{\theta}\Pi_\alpha^{(3)} \right)^T = 0 \tag{62}$$

This *homogeneous* sequence of linear equations, has again a non-singular system matrix, for the same reason mentioned earlier, related to the dispersion relation. As a consequence,

$$\left(U_\alpha^{(1)}, W_\alpha^{(1)}, \frac{\Theta_\alpha^{(2)}}{N\overline{\theta}}, \overline{\theta}\Pi_\alpha^{(3)} \right) = 0 \qquad (\alpha > 2) \tag{63}$$

i.e. the higher-order terms all vanish.

3.2.4 Mean flow

Finally, the mean-flow terms of the Exner pressure equation yield

$$\frac{\partial U_0^{(0)}}{\partial \chi} = 0 \tag{64}$$

i.e. the leading-order mean flow is horizontally homogeneous. From the momentum equations and the entropy equation we obtain, using the fourth component of (54b), the polarization relations from (52), and noticing again that $\overline{\rho} = \overline{P}/\overline{\theta}$, we find

$$\frac{\partial U_0^{(0)}}{\partial \tau} + \overline{\theta}\frac{\partial \Pi_0^{(2)}}{\partial \chi} = -\frac{1}{2\overline{\rho}} \left\{ \frac{\partial}{\partial \chi} \left(\overline{\rho} \left| U_1^{(0)} \right|^2 \right) + \frac{\partial}{\partial \zeta} \left[\overline{\rho}\, \Re \left(U_1^{(0)}\, W_1^{(0)\,*} \right) \right] \right\}, \tag{65a}$$

$$\overline{\theta}\frac{\partial \Pi_0^{(2)}}{\partial \zeta} - \frac{\Theta_0^{(2)}}{\overline{\theta}} + \frac{\left| \tilde{X}_1^{(1)} \right|^2}{2\,\overline{\theta}^2} = -\frac{1}{2\overline{\rho}} \left\{ \frac{\partial}{\partial \chi} \left[\overline{\rho}\, \Re \left(U_1^{(0)}\, W_1^{(0)\,*} \right) \right] + \frac{\partial}{\partial \zeta} \left(\overline{\rho} \left| W_1^{(0)} \right|^2 \right) \right\}, \tag{65b}$$

$$W_0^{(1)} = 0. \tag{65c}$$

The right hand expressions in the two mean-flow momentum equations, (65a) and (65b), represent the influence of the large-scale divergence of the nonlinear momentum fluxes induced by the wave activity. These expressions turn out to be identical in the anelastic and pseudo-incompressible models. The only difference between these models in the mean flow equations is the third term on the right of the vertical momentum equation, (see also Achatz et al., 2010). This wave-induced term is zero for the anelastic equations, while it equals $\left| \Theta_1^{(1)} \right|^2 / 2\,\overline{\theta}^2$ for the compressible and pseudo-incompressible dynamics.

Since the zero-order vertical mean flow $W_0^{(0)}$ vanishes, the vertical momentum equation effectively becomes a hydrostatic balance between the vertical $\Pi_1^{(2)}$ gradient and the mean-flow potential temperature $\Theta_0^{(2)}$, with wave-induced perturbations. Likewise, since the first-order mean-flow potential temperature $\Theta_0^{(1)}$ vanishes, the mean-flow entropy equation (65c) is a diagnostic equation for the, actually vanishing, leading-order mean-flow vertical wind $W_0^{(1)}$ induced by heating due to the, actually vanishing, divergence of the wave related potential-temperature flux.

Given the wave-induced nonlinear terms, (64) and (65) are four equations for as many unknowns, which are $U_0^{(0)}, \Pi_0^{(2)}, \Theta_0^{(2)}$, and $W_0^{(1)}$. Using (64), $\partial U_0^{(0)}/\partial\tau$ can be eliminated from (65a), yielding together with (65b) two coupled linear equations for $\Pi_0^{(2)}$ and $\Theta_0^{(2)}$ which can be solved by standard means. Reinserting $\Pi_0^{(2)}$ into (65a) one then obtains a predictive equation for the mean-flow horizontal wind. Finally, according to (65c) the mean-flow vertical wind vanishes up to and including $O(\varepsilon)$.

4 Conclusions

In this paper we have addressed the formal asymptotics of weakly compressible atmospheric flows involving three asymptotically different time scales for sound, internal waves, and advection. Both the pseudo-incompressible and the Lipps & Hemler anelastic model yield very good approximations to the linearized internal wave dynamics in a compressible flow for realistic background stratifications and on length scales comparable to the pressure and density scale heights. These sound-proof models should be applicable for stratification strengths $(h_{\rm sc}/\overline{\theta})\,(d\overline{\theta}/dz) < O(\varepsilon^{2/3})$, where ε is the flow Mach number. This constraint guarantees the sound-proof and compressible internal waves to evolve asymptotically closely even over advective time scales. For typical flow Mach numbers $\varepsilon \sim 1/30$, this amounts to vertical variations of the mean potential temperature over the pressure scale height of $\Delta\overline{\theta} \sim 30$ K. Considering that $h_{\rm sc} \sim 8.8$ km for $T_{\rm ref} = 300$ K and that typical tropospheric heights are about 10...15 km, the estimate for the validity of the sound-proof models yields realistic potential temperature variations of $\delta\overline{\theta} \sim$ 30...50 K across the troposphere. We have thus provided an explicit estimate for the regime of validity of the considered sound-proof models that considerably extends Ogura & Phillips' original estimate which required $(h_{\rm sc}/\overline{\theta})\,(d\overline{\theta}/dz) = O(\varepsilon^2)$ and implied unrealistically weak background stratifications (for the original derivations, see (Klein et al., 2010)).

Our main conclusion from the second part of the paper is, in line with (Achatz et al., 2010), that the pseudo-incompressible model has the same WKB asymptotics as the compressible Euler equations for internal wave packets with wavelength small compared with the pressure and potential temperature scale heights. This is true even for background potential temperature stratifications of order unity, i.e., for $(1/\overline{\theta})\,d\overline{\theta}/d\zeta = \mathscr{O}(1)$ for vanishing Mach number. In this regime there are differences between the anelastic and pseudo-incompressible models which arise as a consequence of the different divergence constraints enforced by these models and of the nonlinearity of the pressure gradient term that exists only in the compressible and pseudo-incompressible equations. While these effects do *not* affect the dispersion and amplification of a WKB-wavepacket, they do change the generation of higher harmonics and the wave-meanflow interaction.

Interesting future directions of research will be the extension of the WKB theory to three space dimensions, and its embedding in a multiple scales asymptotic theory that couples small-scale internal waves described by WKB with large-scale hydrostatic dynamics. In this context, see also (Shaw and Shepherd, 2008, 2009).

Acknowledgements

The author thanks Nils Wedi for the opportunity to present the main material covered in this paper to a distinguished audience at ECMWF in the fall of 2010, Ulrich Achatz, Fabian Senf, and Piotr Smolarkiewicz for stimulating discussions and challenges, and Deutsche Forschungsgemeinschaft for partial support through grant DFG KL 611/14.

References

Achatz, U., R. Klein, and F. Senf, 2010: Gravity Waves, Scale Asymptotics and the Pseudo-Incompressible Equations. *J. Fluid Mech.*, **663**, 120–147.

Almgren, A. S., J. B. Bell, C. A. Rendleman, and M. Zingale, 2006: Low mach number modeling of type ia supernovae. i. hydrodynamics. *The Astrophysical Journal*, **637**, 922–936.

Bannon, P. R., 1996: On the anelastic approximation for a compressible atmosphere. *Journal of the Atmospheric Sciences*, **53**, 3618–3628.

Bretherton, F. P., 1966: The propagation of groups of internal gravity waves in a shear flow. *Quart. J. Roy. Met. Soc.*, **92**, 466–480.

Davies, T., A. Staniforth, N. Wood, and J. Thuburn, 2003: Validity of anelastic and other equation sets as inferred from normal-mode analysis. *Q. J. R. Meteorol. Soc.*, **129**, 2761–2775.

Durran, D. R., 1989: Improving the anelastic approximation. *Journal of the Atmospheric Sciences*, **46**, 1453–1461.

Durran, D. R., 2010: *Numerical Methods for Fluid Dynamics: With Applications to Geophysics*. 2d ed., Springer, New York, Berlin, Heidelberg, 516 pp.

Dutton, J. A. and G. H. Fichtl, 1969: Approximate equations of motion for gases and liquids. *Journal of the Atmospheric Sciences*, **47**, 1794–1798.

Grimshaw, R., 1975: Internal gravity waves: critical layer absorption in a rotating fluid. *J. Fluid Mech.*, **70**, 287–304.

Hairer, E., C. Lubich, and G. Wanner, 2006: *Geometric Numerical Integration*, Springer Series in Computational Mathematics, Vol. 31. 2d ed., Springer.

Jebens, S., O. Knoth, and R. Weiner, 2009: Explicit Two-Step Peer Methods for the Compressible Euler Equations. *Mon. Wea. Rev.*, **137**, 2380–2392.

Klein, R., U. Achatz, D. Bresch, O. M. Knio, and P. K. Smolarkiewicz, 2010: Regime of Validity of Sound-Proof Atmospheric Flow Models. *J. Atmos. Sci.*, **67**, 3226–3237.

Klemp, J. B., W. C. Skamarock, and J. Dudhia, 2007: Conservative split-explicit time integration methods for the compressible nonhydrostatic equations. *Monthly Weather Review*, **135**, 2897–2913.

Lipps, F. and R. Hemler, 1982: A scale analysis of deep moist convection and some related numerical calculations. *Journal of the Atmospheric Sciences*, **29**, 2192–2210.

Müller, P., 1976: On the diffusion of momentum and mass by internal gravity waves. *J. Fluid Mech.*, **77**, 789–823.

Prusa, J., P. Smolarkiewicz, and A. Wyszogrodzki, 2008: Eulag, a computational model for multiscale flows. *Computers & Fluids*, **37**, 1193–1207.

Reich, S., 2006: Linearly Implicit Time Stepping Methods for Numerical Weather Prediction. *BIT*, **46**, 607–616.

Shaw, T. A. and T. G. Shepherd, 2008: Wave-activity conservation laws for the three-dimensional anelastic and boussinesq equations with a horizontally homogeneous background flow. *J. Fluid Mech.*, **594**, 493–506.

Shaw, T. A. and T. G. Shepherd, 2009: A theoretical framework for energy and momentum consistency in subgrid-scale parameterization for climate models. *J. Atmos. Sci.*, **66 (10)**, 3095–3114.